

Self-healing Dynamic Bond-based Rubbers: Understanding the Mechanisms in Ionomeric Elastomer Model Systems

N. Hohlbein¹, A. Shaaban¹, A. R. Bras², W. Pyckhout-Hintzen², A. M. Schmidt^{1*}

¹ Universität zu Köln, Chemistry Department, Luxemburger Str. 116, D-50939 Cologne, Germany

² Forschungszentrum Jülich, Jülich Centre for Neutron Science-1 and Institute for Complex Systems-1, Wilhelm-Johnen-Straße, D-52428 Jülich, Germany

*E-Mail: annette.schmidt@uni-koeln.de

Electronic Supplementary Information (ESI)

S1 Thermal Properties of the Ionomers

Table S1. Thermal properties of PM-X ionomers as obtained from DSC thermograms.

sample ^a	T_g [°C]	ΔT_g [°C]	T_i [°C]	ΔT_i [°C]	$\Delta C_{p,g}$ [J·g ⁻¹ ·K ⁻¹]	$\Delta C_{p,i}$ [J·g ⁻¹ ·K ⁻¹]
PNa-0.3	-48.0	4.9	-	-	0.295	-
PNa-0.4	-49.2	6.2	-	-	0.362	-
PNa-2.0	-42.6	9.7	-	-	0.388	-
PNa-2.6	-40.2	9.6	58.4	2.5	0.293	3.1E-2
PNa-4.2	-35.9	4.5	45.6	1.0	0.139	3.8E-3
PNa-5.2	-37.8	8.9	56.8	3.1	0.216	3.0E-2
PNa-6.2	-34.7	10.4	82.8	6.4	0.198	1.4E-2
PNa-8.6	-33.6	10.5	123.0	8.4	0.192	1.8E-2
PNa-9.2	-34.5	13.8	126.4	7.4	0.196	2.8E-1
PNa-9.9	-34.0	21.4	122.0	8.2	0.31	1.8E-2
PZn-0.3	-48.0	5.2	-	-	0.314	-
PZn-0.4	-48.9	5.9	-	-	0.276	-
PZn-2.0	-43.7	10.0	-	-	0.396	-
PZn-2.6	-40.3	9.1	58.3	2.2	0.332	2.4E-2
PZn-4.2	-37.7	7.5	67.5	1.3	0.278	3.9E-2
PZn-5.2	-37.7	6.3	66.5	3.2	0.242	1.7E-2
PZn-6.2	-36.2	14.3	67.5	6.4	0.306	7.6E-2
PZn-8.6	-34.6	10.6	150.6	8.6	0.274	1.8E-2
PZn-9.2	-33.3	19.8	148.9	7.8	0.304	1.0E-1
PZn-9.9	-31.5	17.3	152.7	8.3	0.288	3.9E-2
PCo-0.3	-47.9	6.3	-	-	0.324	-
PCo-0.4	-48.6	5.7	-	-	0.318	-
PCo-2.0	-40.7	9.7	-	-	0.329	-
PCo-2.6	-40.5	9.3	50.4	3.9	0.316	3.4E-2
PCo-4.2	-39.5	9.4	53.8	1.5	0.278	4.2E-3
PCo-5.2	-40.0	8.6	45.5	3.4	0.234	4.4E-2
PCo-6.2	-36.8	9.6	48.9	5.3	0.193	3.9E-2
PCo-8.6	-36.8	16.1	95.3	8.3	0.360	2.3E-1
PCo-9.2	-33.6	14.4	135.0	11.8	0.210	3.3E-2
PCo-9.9	-33.8	20.1	142.8	9.6	0.299	1.7E-2

^a T_g : glass transition temperature (point of inflection), ΔT_g : width of the glass transition, T_i : transition temperature of the ion-rich phase, ΔT_i : width of the transition, $\Delta C_{p,g}$: heat capacity change at T_g , $\Delta C_{p,i}$: heat capacity change at T_i .

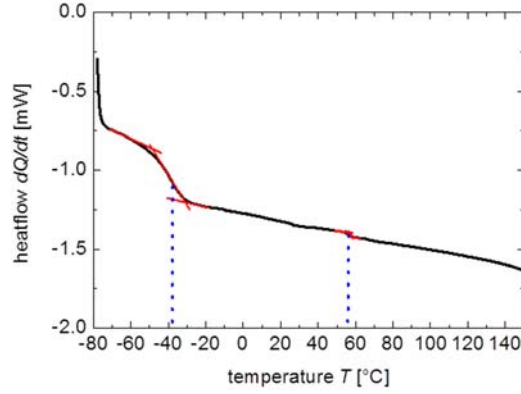


Figure S1. Typical DSC thermogram of PNa-5.2 (second heating run).

S2 Details of the SAXS analysis

Since the particle size distribution is neither known nor can be predicted a priori from the chemical building-up of the ionic clusters, we have assumed a normalized Gaussian distribution of the ionic cluster aggregate radius R with weight w as

$$w(R) = \frac{1}{\sqrt{2\pi\sigma^2}} \exp\left(-\frac{(R-R_m)^2}{2\sigma^2}\right) \quad (\text{eq. S1})$$

Here, R_m is the mean radius of the distribution, and σ the standard deviation. Thus, the form factor $\langle P(q) \rangle_R$ of the multiplet including polydispersity is

$$\langle P(q) \rangle_R = \frac{\int_0^{\infty} w(R) (4\pi/3) R^3 \left(\frac{3(\sin(qR) - qR \cos(qR))}{(qR)^3} \right)^2 dR}{\int_0^{\infty} w(R) dR} \quad (\text{eq. S2})$$

The integrals are calculated numerically, and the upper limit set to $\sim 20 \sigma$. Although the distribution is normalized by definition, possible errors due to the truncation of the summation are divided out. The total scattering intensity $I(q)$ then amounts to

$$I(q) = A \langle P(q) \rangle_R S(q)_{PY/PC} + I_{bg} + Bq^{-4} \quad (\text{eq. S3})$$

with A being a lumped prefactor absorbing the uncertainties of the calibration, concentration and contrasts, I_{bg} an in the present q -range constantly taken diffuse background, and B/q^4 mainly parasitic forward scattering intensity, respectively. The square brackets point at the averaging over the size distribution.

For the structure factor $S(q)_{PY/PC}$ i.e. Percus-Yevick (PY) or paracrystal (PC), we employ the usual additional assumption that the interaction is locally monodisperse, using the mean size of the aggregate R_m . The Percus-Yevick structure factor has been reported on already numerous times, and we refer for the details to the literature.¹⁻⁴ For our purpose we here only report the radius of the equivalent hard sphere interaction radius $R_{d,PY}$ ($= D/2$) and the fitted volume fraction of the aggregates ν_m (Table 2 in the main article).

The paracrystalline structure factor was introduced by Matsuoka et al (1987) for related microphase-separated systems, and calculates the interference functions depending on a chosen crystalline lattice configuration. We refer to the literature for the exact lengthy expressions.^{5,6} For the present study, we add the lattice parameter constant a and their Gaussian-distributed distortion $\Delta a/a$ as additional

parameters. The size R_m and distribution of the ionic aggregates that occupy the vertices i.e. lattice points are common in both approaches.

$R_{d,PC}$ is calculated as the distance at which the particles are to touch each other from simple geometric considerations; while the line of contact in the simple cubic (sc) model is along the edges of the lattice unit and yields $R_{d,PC}(sc) = a/2$, in the body-centered cubic (bcc) model this line corresponds to the diagonal of the cubic lattice cell with $R_{d,PC}(bcc) = \frac{\sqrt{3}}{4} \cdot a$. For the face-centered cubic (fcc) model, the relation becomes $R_{d,PC}(fcc) = \frac{\sqrt{2}}{4} \cdot a$.

S3 Mechanical Properties of the Ionomers

Table S2. Results of the mechanical characterization of the ionomers by oscillating rheology and tensile tests.

sample ^a	G'_N [MPa]	τ_D [s]	ϵ_R [%]	σ_{max} [MPa]	E_{neu} [MPa]
PNa-0.3	0.06	n. d.			
PNa-0.4	0.05	n. d.			
PNa-1.9	0.23	8.0×10^{-2}			
PNa-2.6	0.56	2.03			
PNa-4.2	0.60	2.25			
PNa-5.2	0.93	3.25	349 ± 56	1.75 ± 0.16	2.41 ± 0.19
PNa-6.2	1.03	3.55	335 ± 34	0.77 ± 0.01	2.54 ± 0.17
PNa-8.6	1.17	9.67	197 ± 9	2.23 ± 0.17	3.88 ± 0.68
PNa-9.2	2.05	n. d.	276 ± 53	1.01 ± 0.18	2.90 ± 0.34
PZn-0.3	0.07	1.0×10^{-2}			
PZn-0.4	0.06	n. d.			
PZn-1.9	0.17	1.5×10^{-1}			
PZn-2.6	0.36	8.43			
PZn-4.2	0.42	24.2			
PZn-5.2	1.46	4.19×10^2	265 ± 31	1.43 ± 0.06	2.62 ± 0.17
PZn-6.2	1.70	1.57×10^2	244 ± 19	2.40 ± 0.40	3.61 ± 0.44
PZn-8.6	2.59	n. d.	227 ± 44	1.87 ± 0.08	5.59 ± 0.22
PZn-9.2	5.39	n. d.	50 ± 3	2.83 ± 0.11	7.44 ± 0.26
PZn-9.9	6.34	3.31×10^4	52 ± 6	3.85 ± 0.28	8.18 ± 0.35
PCo-0.3	0.08	1.0×10^{-2}			
PCo-0.4	0.05	n. d.			
PCo-1.9	0.28	4.83×10^2			
PCo-2.6	0.48	3.14×10^3			
PCo-4.2	0.83	n. d.			
PCo-5.2	1.11	1.43×10^4	217 ± 42	1.49 ± 0.23	2.64 ± 0.13
PCo-6.2	1.47	n. d.	136 ± 26	2.83 ± 0.63	4.64 ± 0.58
PCo-8.6	2.13	n. d.	42 ± 18	2.08 ± 0.99	6.33 ± 0.28
PCo-9.9	5.89	n. d.	202 ± 8	4.91 ± 0.25	7.18 ± 0.11

^a G'_N : levelled-off storage modulus from rheology; ϵ_R : elongation at break, σ_{max} : tensile strength, E : elastic modulus from tensile experiments.

S4 References

1. D. J. Kinning and E. L. Thomas, *Macromolecules*, 1984, **17**, 1712–1718.
2. D. J. Yarusso and S. L. Cooper, *Macromolecules*, 1983, **16**, 1871–1880.
3. J.-P. Hansen and I. R. McDonald, *Theory of simple liquids*, Academic Press, London, 2nd edn., 1986.

4. F. J. Stadler, W. Pyckhout-Hintzen, J.-M. Schumers, C.-A. Fustin, J.-F. Gohy, and C. Bailly, *Macromolecules*, 2009, **42**, 6181–6192.
5. H. Matsuoka, H. Tanaka, N. Iizuka, T. Hashimoto, and N. Ise, *Phys. Rev. B*, 1990, **41**, 3854–3856.
6. H. Matsuoka, H. Tanaka, T. Hashimoto, and N. Ise, *Phys. Rev. B*, 1987, **36**, 1754–1765.